

Host Exclusion and Coexistence in Apparent and Direct Competition: An Application of Bifurcation Theory

J. V. Greenman¹ and P. J. Hudson

Stirling Mathematical Ecology Group, University of Stirling, Stirling FK9 4LA, Scotland

E-mail: j.v.greenman@stir.ac.uk, p.j.hudson@stir.ac.uk

Received March 3, 1998

Recent empirical studies have focused attention on the interplay in multi-host systems of parasite-mediated apparent competition and direct competition between hosts. However, theoretical investigation of such systems has been hindered by the onset of algebraic intractability with the increase in system dimensionality. In this paper we circumvent this problem by using a geometric approach in which arrays of bifurcation maps are constructed, each map being structured by the set of (bifurcation) points in parameter space at which qualitative changes in system behaviour take place. From these maps can be compiled a concise catalogue of the possible modes of system behaviour, enabling an investigation of the interaction of apparent and direct competitive forces to be carried out. Of importance is the identification of those situations where increasing one or both of these competitive forces leads to a change in the stability state. The maps provide an efficient way of determining whether, and, if so, under what conditions, specific modes of behaviour are allowed by the model. Two field phenomena of particular interest, discussed in the paper, are host invasion and dominance reversal resulting from the introduction of the pathogen into a directly competitive system. © 1999 Academic Press

INTRODUCTION

Empirical and theoretical studies have highlighted the important role that parasites can play in the population dynamics of their host (Anderson and May, 1991; Scott and Smith, 1994; Grenfell and Dobson, 1995). Since, certainly in the case of directly transmitted viral or bacterial infections, transmission is invariably a function of the size of the susceptible host population, elimination of the host is a rare occurrence, with regulation by pathogen or capacity constraint the most likely outcome. One mechanism by which host elimination can occur is through the sharing of the pathogen by a second host, thereby creating a reservoir of infection (Holt and Pickering, 1985). In this situation the system behaves as if there were competition between the hosts (Holt and

Lawton, 1994; Hudson and Greenman, 1998). We will refer to this form of competition as “parasite-mediated apparent competition” to distinguish it from “direct competition between hosts,” a category that includes competition for limited resources (Murray, 1993).

There is a wealth of examples in the literature invoking parasite-mediated apparent competition. Interestingly, these examples show a wide range of variation in the way in which the pathogen can act. For example, transmission rates between species can vary according to habitat structure so that a vulnerable species can be excluded from one habitat by the reservoir species but still persist in another habitat. This appears to be the case for the gut nematode *Graphidium strigoum* that occurs in both hares and rabbits in the Netherlands but is more virulent in hares. Development and transmission of the parasite is favoured in shady woodlands so transmission to hares is faster and exclusion from such habitats takes place (Broekhuizen and Kememrs, 1976).

¹ To whom correspondence should be addressed.

The ecological conditions that may favour one species invading the habitat of a second species may lead to the introduction of a pathogen to the vulnerable resident species. For example, domestic dogs act as a reservoir for rabies which they may transmit to endangered carnivores, including wild dogs, Ethiopian wolf, and Burnetts fox (MacDonald, 1993), thereby reducing their numbers further. Further, a pathogen may debilitate a resident population and allow invasion of a second species that was previously excluded by direct competition between hosts. A recent study in South Africa indicates that the impact of a trematode parasite on an indigenous mussel reduces both the growth and the (direct) competitive ability of the mussel and may have allowed invasion by the European mussel, *Mytilus galloprovincialis* (Calvo-Ugarteburu and McQuaid, 1997).

There is also some evidence that a parasite may influence the outcome of direct competition between hosts. In India the simian malarial parasite *Plasmodium knowlesi* is highly pathogenic to the rhesus monkey (*Macaca mulatta*) and excludes the monkey from Eastern India and Bangladesh. In these areas a more resistant macaque (*M. fuscularis*) is present but this species is a weaker competitor in the absence of the pathogen, in which case it is excluded by the rhesus monkey (Allison, 1982).

These studies illustrate the wealth of interactions that can be observed in multi-host shared-pathogen systems. However, the findings are seldom conclusive since in very few of the studies has it been possible to separate out the effects of the two forms of competition: (parasite-mediated) apparent competition and direct competition (between hosts). One recent exception is the laboratory study carried out by Bonsall and Hassell (1997) on the effect of a parasitoid wasp on lepidopteran larvae. They demonstrated clearly that apparent competition can lead to host exclusion, with obvious implications for biodiversity. There is also the classic experiment of Park (1948) examining the influence of the sporozoan parasite *Adelina tribolii* on two flour beetles: *Tribolium confusum* and *T. castaneum*. In the absence of the pathogen, *T. confusum* invariably dominated but in the presence of the pathogen the result was reversed. In single-host infections *T. castaneum* populations were reduced while *T. confusum* populations were not. In effect the sporozoan is more pathogenic in the dominant competitor so that, when the two species are present, the pathogen reduces the competitive ability of the dominant species and reverses the outcome of the contest.

Insight into the dynamics of multi-host shared-pathogen systems has been provided by the local analysis

of particular mathematical models. Holt and Pickering (1985) used the basic susceptible–infecteds (S–I) model of a directly transmitted microparasite, shared between hosts that do not exhibit lasting immunity, to explain the phenomenon of host exclusion and they gave conditions under which this occurs. This model has subsequently been extended to include density dependence (Begon and Bowers, 1992), free living stages (Begon and Bowers, 1994, 1995), and direct (between hosts) competition (Anderson and May, 1986; Bowers and Turner, 1997). Macroparasite models have also been used to investigate the interaction of different forms of competition (Greenman and Hudson, 1997c; Yan, 1996).

One major problem with these models is algebraic intractability which prevents a full analytic treatment from being given. One way around this difficulty is to take a geometric approach, focusing on the “bifurcation” points in parameter space, for which there is a qualitative change in system behaviour (Wiggins, 1990). The basic type of bifurcation is the transcritical bifurcation in which two equilibrium trajectories collide in state space (the space of the population densities) as a bifurcation point is encountered while travelling along a path in parameter space. In such a bifurcation two phenomena typically occur. As a result of the collision one equilibrium becomes (biologically) relevant and the two equilibria exchange stability states. The equilibrium that is relevant throughout the collision process is said to act as a “gate” for the emerging equilibrium and endows it with stability, becoming unstable itself in the process. Because of this property the approach taken in this paper has been referred to as gateway analysis (Greenman and Hudson, 1997b). Besides the transcritical bifurcation, Hopf and saddle-node bifurcations can also be present and often must be present to provide a consistent bifurcation structure.

This structure can be represented geometrically on a “bifurcation map” in parameter space, showing how the curves of bifurcation points intersect. The complexity in structure that emerges derives from the variety of ways in which the relatively simple bifurcation curves intersect and not from the complexity of those curves themselves. The maps provide an overview of the system and a concise catalogue of possible dynamical modes of behaviour. The most important of these will be discussed in the last section of the paper. Methods for constructing these maps will be explained in the context of the density-dependent S–I model, extended to include direct (between-host) competition, adding to (parasite-mediated) apparent competition, already built into the model.

THE TWO-HOST S–I MODEL WITH APPARENT AND DIRECT COMPETITION

The extended two-host susceptible–infected model is defined by the equations ($i = 1, 2; j \neq i$)

$$dH_i/dt = H_i(r_i - \theta_i H_i - \phi_i H_j) - \alpha_i Y_i \quad (1a)$$

$$dY_i/dt = X_i(\beta_{ii} Y_i + \beta_{ij} Y_j) - d_i Y_i. \quad (1b)$$

For host i , X_i is the susceptible, Y_i the infected, and $H_i = X_i + Y_i$ the total population density. The definitions and meanings of the model parameters and dimensionless coefficients are given in Table I. In particular, r_i is the net natural birth rate (at low densities), α_i is the infection-induced mortality rate, and d_i is the “loss” rate from the infected state due to mortality (natural and infection-induced) and recovery. Further, parameter θ_i is a measure of density dependence (with $\theta_i = r_i/K_i$, where K_i is the carrying capacity) and ϕ_i is a measure of the strength of direct competition experienced by host i . Throughout the analysis we will consider only those situations in which both hosts have a positive net natural birth rate (i.e., $r_i > 0$) and the pathogen is capable of regulating each host when alone (i.e., $\alpha_i > r_i$). We will also ignore the effect of infection on fecundity.

The behaviour of Model (1a), (1b) will be investigated in three stages: (i) with no infection ($\beta_{ij} = 0; i, j = 1, 2$), (ii) with no direct competition ($\phi_i = 0, i = 1, 2$), and (iii) with both infection and direct competition. The analysis will be a local analysis, focusing on behaviour close to the

stationary states of the model, represented by its equilibrium points in state space. For each equilibrium (point) there are two important issues: whether the equilibrium is relevant and whether it is stable. By relevance we mean biological relevance in that all population densities, evaluated at that equilibrium, are non-negative. By stable we mean that the system will always return to the equilibrium state under small perturbations. For this to happen, all eigenvalues of the system Jacobian matrix, evaluated at the equilibrium in question, must have a negative real part.

The behaviour of the model is well known when there is no infection (Murray, 1993) and can be expressed simply in terms of the dimensionless indices: $v_i = \phi_i K_j / r_i$ ($j \neq i$). There are three equilibria of interest: the always relevant single-host equilibria with one of the hosts at carrying capacity limit and the other absent,

$$(H_1, Y_1, H_2, Y_2) = (K_1, 0, 0, 0), (0, 0, K_2, 0),$$

and the coexistence equilibrium (with both hosts present),

$$(H_1, Y_1, H_2, Y_2) = (K_1 \xi_1, 0, K_2 \xi_2, 0),$$

where $\xi_i = (1 - v_i)/(1 - v_1 v_2)$, (2)

which is relevant only when either both competitive forces are weak (i.e., $0 < v_i < 1, i = 1, 2$) or both are strong (i.e., $v_i > 1, i = 1, 2$). In the first case coexistence is the only stable equilibrium of the system but it is unstable in the second. In all other cases at least one of the single-host equilibria is stable, with exclusion of the other host.

TABLE 1

The Basic S–I Model Parameters

Model parameters for host i ($i, j = 1, 2$)

a_i = natural birth rate (at low densities)
 α_i = infection-induced mortality rate
 γ_i = recovery from infection rate
 ϕ_i = direct (between-host) competition coefficient
 $d_i = \alpha_i + b_i + \gamma_i > \alpha_i$

Dimensionless coefficients ($j \neq i$)

$c_{1i} = \alpha_i / r_i$ (assumed > 1)
 $s_0 = r_2 / r_1$
 $v_i = \phi_i K_j / r_i$
 $S_{0i} = c_{3i}(c_{1j} - 1)/(c_{1i} - 1)$

Dimensionless state variables

$h_i = H_i / K_i$

b_i = natural death rate
 $K_i = r_i / \theta_i$ = carrying capacity
 β_{ij} = infection transmission coefficients

$r_i = a_i - b_i$ (assumed > 0)

$c_{2i} = d_i / r_i, \quad c_{2i} > c_{1i}$
 $c_{3i} = (\beta_{ji} / \beta_{ii})(d_i / d_j)$
 $\xi_i = (1 - v_i)/(1 - v_1 v_2)$
 $R_{0i} = (\beta_{ii} K_i) / d_i$

$y_i = (\beta_{ii} / d_i) Y_i$

RELEVANCE AND STABILITY MAPS WITH NO DIRECT COMPETITION PRESENT

The situation in which infection is present, but there is no direct competition ($v_i = 0$, $i = 1, 2$), has been fully analysed by Greenman and Hudson (1997b), who showed that the situation is more complicated than had originally been thought (Holt and Pickering, 1985; Begon and Bowers, 1992). There are six equilibria of interest, characterised by whether there is one host or no host absent and whether the infection is or is not present. The uninfected equilibria are always relevant with the host densities at their capacity limits or zero. The uninfected single-host equilibria are not stable. Invasion by the other host is always possible (when $r_i > 0$) and invasion by the pathogen is possible above threshold, i.e., for $R_{0i} > 1$, where host i is the host present and R_{0i} is its basic reproductive number (Anderson and May, 1991):

$$R_{0i} = \beta_{ii} K_i / d_i.$$

The uninfected coexistence equilibrium is stable when

$$(R_{01}^{-1} - 1)(R_{02}^{-1} - 1) > (\beta_{12}\beta_{21})/(\beta_{11}\beta_{22}) \quad (3)$$

and unstable, with invasion by the pathogen, when the inequality is reversed. These properties can all be established by standard techniques (Murray, 1993).

The properties of the infected equilibria are more complicated. The infected host 1 equilibrium (with host 2 absent) is relevant only when $R_{01} > 1$. Below this threshold at least one of the population densities is negative. Above threshold this equilibrium is stable (with host 2 unable to invade) only for $R_{01} > R_{01}^* > 1$, where

$$R_{01}^* = (1 + (S_{01}(\alpha_1/r_1 - 1))^{-1})^2 / (1 - S_{01}^{-1}) \quad (4)$$

and

$$S_{01} = (\beta_{21}/\beta_{11})(A_2/A_1),$$

$$\text{where } A_i = (\alpha_i/r_i - 1)/d_i. \quad (5)$$

(See the Appendix for proof.)

These various properties can be represented on the “map” of Fig. 1a where a cross section of parameter space in the “variables” R_{0i}^{-1} has been taken. We choose to work with the inverses of R_{0i} to simplify the geometry and to ensure that the region of pathogen persistence is close to the origin. On this map the infected host 1 equilibrium is relevant only to the left of the vertical line

$R_{01}^{-1} = 1$ and stable only to the left of the vertical line $R_{01}^{-1} = R_{01}^{*-1} < 1$. This second line will be referred to as line L_1 .

It is clear from (4) that there can be stability only if $S_{01} > 1$, otherwise R_{01}^* would be negative and the stability condition would not be met. If S_{01} were less than one, therefore, line L_1 would not be present and the equilibrium, at all points to the left of the line, $R_{01}^{-1} = 1$, would be relevant but not stable. We refer to S_{01} and its host 2 companion, S_{02} , as the host “exclusion” indices. They are proportional to the cross-infection coefficients β_{ji} ($j \neq i$) while the basic reproductive numbers, R_{0i} , are proportional to the within-host infection coefficients, β_{ii} .

The map of Fig. 1b shows the shaded relevance and stability regions for the infected host 2 equilibrium when $S_{02} > 1$ with line L_2 , marking the boundary between host 1 exclusion and invasion. We say that L_2 is active when $S_{02} > 1$ since it then intersects the positive orthant ($R_{0i} > 0$, $i = 1, 2$) of R_{0i}^{-1} space. In Figs. 1a and 1b the relevance and stability regions for the two equilibria have been explicitly labelled. For later use, we have also introduced a more concise labelling in which a pair of integers ($p q$) is associated with each region on each map. The first integer, p , specifies how many relevant equilibria of the given type exist for points in that region and the second integer, q , specifies how many of these equilibria are stable. For example, for points in the region labelled (1 0) in Fig. 1a (i.e., the region $R_{01}^{*-1} < R_{01}^{-1} < 1$) the single infected host 1 equilibrium is unstable (i.e., host 2 can invade) while the integer pair (1 0) in Fig. 1b identifies the region ($R_{02}^{*-1} < R_{02}^{-1} < 1$) where the single infected host 2 equilibrium is unstable (i.e., host 1 can invade). An integer pair ($p q$) carries relevance and stability information about a particular equilibrium in a particular region of its map cross section. As shown by the example above, in general a given integer pair identifies different regions on the maps of different equilibria.

One question unanswered by the maps of Figs. 1a and 1b is what happens when the other host invades: will there be infected coexistence or will the “other” host exclude the first host? This question is addressed in Fig. 1c, where the relevance and stability regions for the infected coexistence equilibrium are shown (when $S_{0i} > 1$, $i = 1, 2$). The boundary of its relevance region consists of the lines L_1 and L_2 and the hyperbola defined by (3) with equality, an equation that we will refer to in an obvious notation as ($3 =$). For points in the upper part of this relevance region the equilibrium is stable while in the lower part it is unstable.

Comparing the maps of Fig. 1 we can follow through the consequences of host invasion, supposing that there is eventual convergence to a point equilibrium as

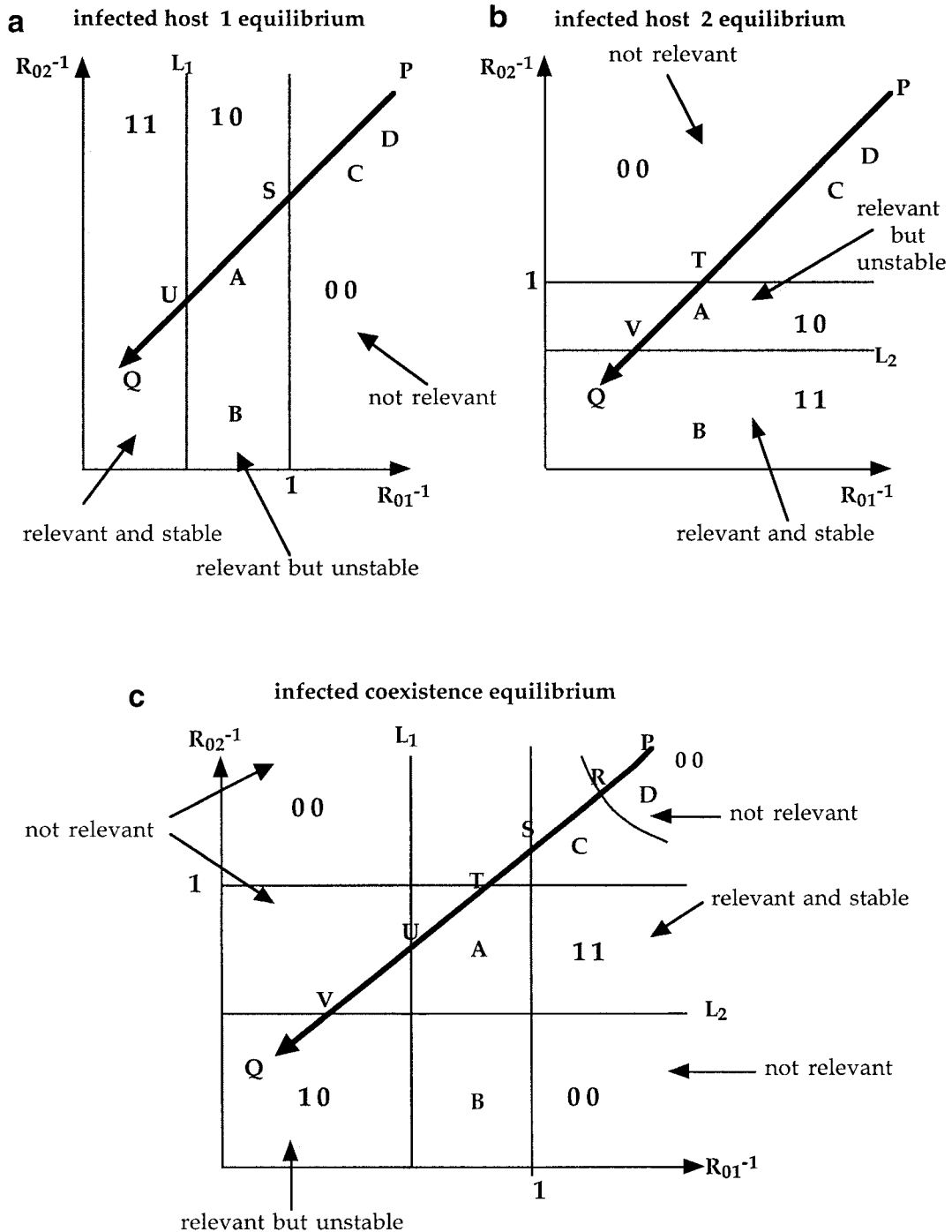


FIG. 1. The bifurcation maps for the infected single-host equilibria (a, b) and the infected coexistence equilibrium (c) when both L_1 and L_2 lines are active and there is no direct competition (i.e., $v_i = 0$). Shown shaded are the relevance regions and the stable and unstable subregions. For each region of each map the relevance and stability properties of the equilibrium associated with that map are summarised succinctly in a double integer notation; (p, q) . p denotes the number of equilibria of the given type that are relevant for points in that region and q is the number of these that are stable. For example, in region (1 1) in (a) there is one relevant infected host 1 equilibrium and it is stable (i.e., host 2 is excluded). In region (0 0) of (a) there is no relevant infected host 1 equilibrium. In general, a given integer pair refers to different regions on different maps. The “dual” property of lines L_1 and L_2 , relating stability for one equilibrium and relevance for another, is evident from a comparison of the map structures, as is the equality of stability states across these boundaries. The path $P \rightarrow Q$ relates to Fig. 2, where the equilibrium trajectories generated by movement along this path are shown. The biological interpretation of points A, B, C , and D is given in the text.

suggested by simulation. For points A , B , C , and D in Fig. 1, for example, we draw the following conclusions:

(i) For the model defined by point A in Fig. 1 all three infected equilibria are relevant but only the coexistence equilibrium is stable. If the system is perturbed from the initial state with host 2 absent but infection present (i.e., from the equilibrium of Fig. 1a) then host 2 will invade and coexistence will follow, with the pathogen still present (Fig. 1c). For the model defined by point B , the coexistence state is no longer an option since this equilibrium has ceased to be relevant. Host 2 invasion will therefore lead to host 1 exclusion (Fig. 1b).

(ii) For the model defined by point C the system is below threshold for pathogen invasion of either host when alone but above threshold for pathogen invasion when the hosts coexist. Perturbing the state with host 1 alone (with the other host and pathogen absent, i.e., in the uninfected host 1 equilibrium state) will lead to invasion by both the other host and the pathogen (Fig. 1c). For point D the other host will invade but not the pathogen, so there will be uninfected coexistence (Fig. 1c).

Examination of the maps of Figs. 1a, 1b, and 1c reveals the existence of certain relationships involving relevance and stability:

(i) Each curve on these maps serves a dual purpose, being a stability boundary for one equilibrium and a relevance boundary for another. For example, the hyperbola ($3 =$) is part of the relevance boundary for the infected coexistence equilibrium and the stability boundary for the uninfected coexistence equilibrium.

(ii) Across each of these curves there is equality of stability state for the two equilibria sharing that boundary. For example, above the hyperbola ($3 =$) the uninfected coexistence equilibrium is stable while below, the infected coexistence equilibrium is stable.

BIFURCATION STRUCTURE WITH NO DIRECT COMPETITION PRESENT

To gain a deeper understanding of these relationships it is necessary to investigate how the equilibria move in state space as paths are traced out in parameter space. Consider, for example, the path $P \rightarrow Q$ shown in Fig. 1. As the hyperbola is crossed at point R in Fig. 1c the trajectories of the infected and uninfected coexistence equilibria collide in state space (Fig. 2). Before the collision the uninfected equilibrium is stable while the infected

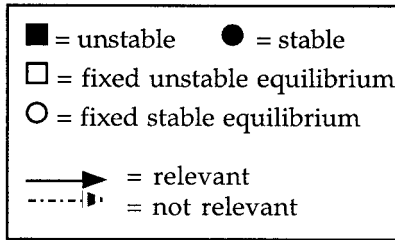
equilibrium is unstable and not relevant. After the collision the uninfected equilibrium has become unstable and the infected equilibrium, both stable and relevant. The uninfected equilibrium acts as a “gateway” for the infected equilibrium into the relevance region and endows it with stability. This is an example of a transcritical bifurcation and the maps such as those shown in Fig. 1, which mark the occurrence of this and other types of bifurcation, will be called “bifurcation maps.”

Crossing point U on the boundary line L_1 , further down the path $P \rightarrow Q$, generates a second transcritical bifurcation with the infected coexistence equilibrium exiting through the infected host 1 gate, transferring its stability to this single-host equilibrium (Fig. 2). This stability switching is recorded on the bifurcation map for the infected host 1 equilibrium shown in Fig. 1a. Returning to Fig. 1c and following path $P \rightarrow Q$ beyond point U , a third transcritical bifurcation occurs at point V on line L_2 . In this case a second infected coexistence equilibrium enters through the infected host 2 gate. After emerging, the coexistence equilibrium is unstable, having transferred its stability to the single-host equilibrium (Fig. 2). This stability switching is indicated on the bifurcation map for the infected host 2 equilibrium shown in Fig. 1b.

At each point of the “bifurcation” curves L_1 and L_2 and the hyperbola ($3 =$) there is a change in stability for both equilibria involved but this stability switching does not always occur. Two examples of this not happening can be found in Figs. 1a and 1b. Point S on the line $R_{01} = 1$ defines a transcritical bifurcation in which an infected host 1 equilibrium emerges through the uninfected host 1 gate (Fig. 2). Neither equilibrium is stable before or after the collision. In fact they are both unstable with respect to host invasion. Similar behaviour occurs at point T on the line $R_{02} = 1$ for host 2 (Fig. 2). In general, if one equilibrium is stable just before collision then stability switching will take place but if neither are stable just before collision then neither will be immediately afterwards (Greenman and Hudson, 1997b).

Transcritical bifurcations correspond to threshold transitions, a familiar topic in the epidemiological literature, although it is unusual for bifurcation terminology to be used explicitly in their description. The change in behaviour that occurs when a change in parameter value takes the system above threshold reflects the fact that a newly emerged point equilibrium has smoothly taken over the role of carrier for the stable state of the system. This interpretation holds even if the transition involves a single host (e.g., the familiar threshold condition for pathogen invasion: $R_{01} > 1$) provided that attention is restricted to the one-host submodel in which the

State Space Equilibrium Trajectories



use_i = uninfected host i equilibrium
 ise_i = infected host i equilibrium
 uce = uninfected coexistence equilibrium
 ice = infected coexistence equilibrium
 At (S) collision between use_1 and ise_1
 At (T) collision between use_2 and ise_2

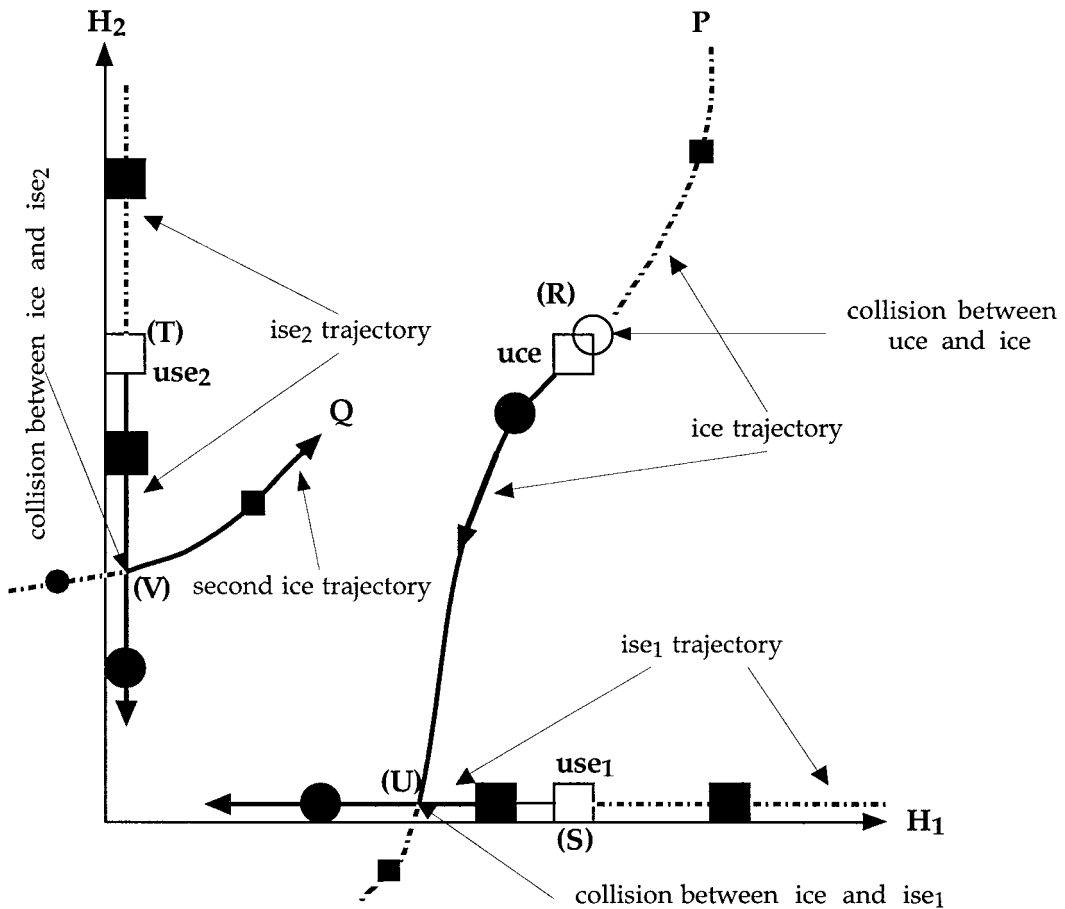


FIG. 2. The infected single and coexistence equilibrium trajectories generated by movement along the path $P \rightarrow Q$ of Fig. 1. The trajectories are shown in the cross section of state space defined by the host densities H_1 and H_2 . For given K_i the uninfected equilibria are fixed. Two equilibria collide at their trajectory intersection, to generate a transcritical bifurcation. The sequence of bifurcations as path $P \rightarrow Q$ is followed is indicated by a common point labelling in Figs. 1 and 2. The trajectory sections are coded according to relevance and stability to illustrate the phenomena of stability switching and gateway emergence.

Infected Coexistence Bifurcation Map - Saddle Node Bifurcations

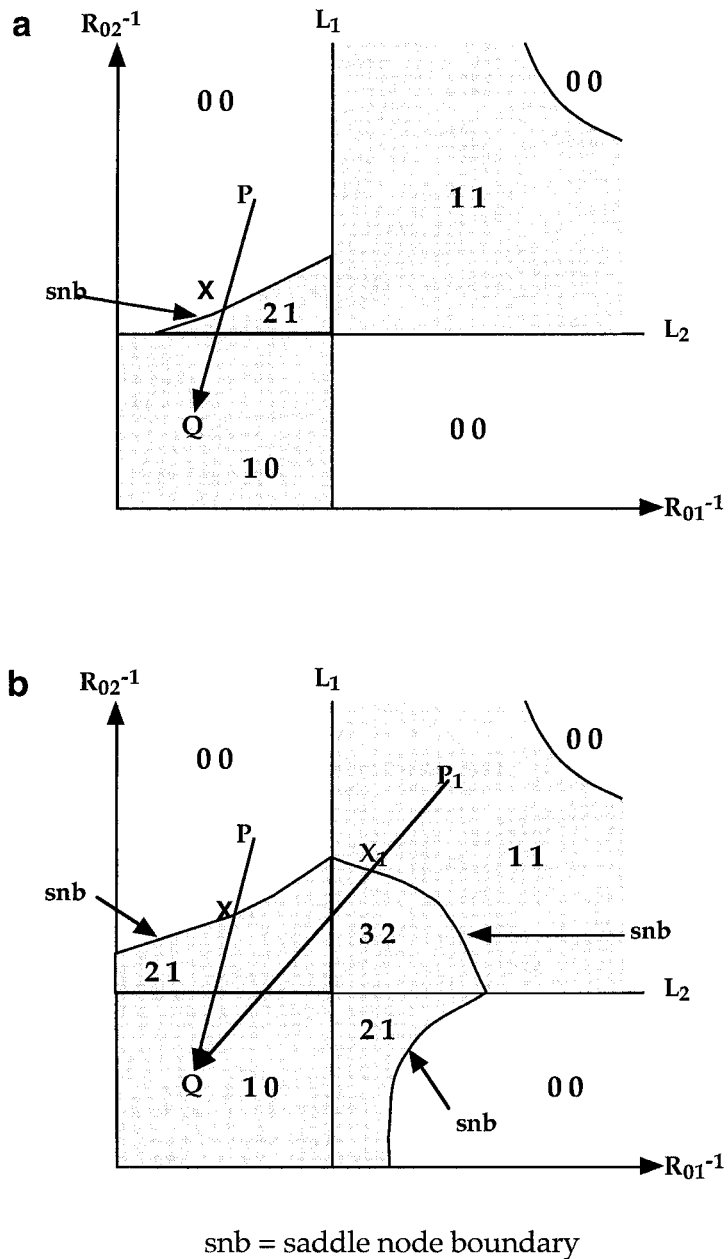


FIG. 3. Saddle-node bifurcation associated with the intersection of active L_1 and L_2 lines on the infected coexistence bifurcation map. In (a) is shown the “asymmetric” solution to the singularity “dilemma” and in (b) is shown the “symmetric” solution. At typical points X and X_1 at the intersection of the saddle-node boundaries and the paths $P \rightarrow Q$ and $P_1 \rightarrow Q$ a pair of infected coexistence equilibria is created, one stable and the other unstable.

other host is absent. For this submodel there is indeed stability switching but not for the full model.

Complications: The Emergence of Saddle-Node Bifurcations

The bifurcation map for the infected coexistence equilibrium in Fig. 1c is, in fact, incomplete. If two transcritical curves involving a particular type of equilibrium intersect (for example, L_1 and L_2 in Fig. 1c) then multiple equilibria of that type have to be present. If this were not the case then crossing to a path just below the point of intersection from a path just above would result in a jump in the trajectory from one gate to another on different axes. There are two solutions to this “singularity” dilemma. In the first (Fig. 3a), one infected coexistence equilibrium enters through one of the infected single-host gates while a second exits through the other gate. Crossing from one path to another across the intersection point merely reorders this sequence of events. If entry occurs before exit then there are two infected coexistence equilibria present. If the sequence is reversed then none are present (Fig. 3a). In the second solution (Fig. 3b) three infected coexistence equilibria have become relevant. The two stable equilibria exit through the infected single-host gates while the third unstable equilibrium remains.

Multiple equilibria can arise in two ways: by entry through a transcritical gate to add to an existing relevant equilibrium, as we have just seen, or by saddle-node bifurcation. This second mechanism can be observed in action as path $P \rightarrow Q$ is traced out in Figs. 3a and 3b. As we enter the relevance region of the infected coexistence equilibrium at point X , two equilibria suddenly appear, arriving together from complex state space and then separating in real state space. A saddle-node bifurcation need not occur on the boundary of a relevance region but can occur within that relevance region as Fig. 3b shows. In the saddle-node examples shown in Figs. 3a and 3b one of the pair of equilibria created is stable while the other is unstable, but this is not always the case (Greenman and Hudson, 1997b).

The saddle-node bifurcation is not a familiar structure in the taxonomy of biological behaviour. The overall effect, however, is similar to that of the transcritical bifurcations defined by the lines L_i . If the saddle-node bifurcation with a stable, unstable pair is “run” backwards then host exclusion is likely to emerge from host coexistence as the threshold (e.g., point X in Fig. 3a) is crossed. The two bifurcations differ in the way this is brought about. In the transcritical bifurcation the transition is smooth

with the stability transferred to the single-host equilibrium with which collision takes place. For the saddle-node bifurcation the transition is not so smoothly accomplished since the equilibrium with which it collides also ceases to be relevant. Beyond the saddle-node threshold the system has to seek out an alternative stable equilibrium state in a different part of state space. For Fig. 3a the only candidate is the infected host 1 equilibrium. Whether the system actually converges to this equilibrium depends on the global rather than the local properties of the model.

The existence of saddle-node bifurcations is one of the reasons why the conjectures made by Holt and Pickering (1985) and Begon and Bowers (1992) sometimes fail. The conjecture that there can be at most one relevant stable infected coexistence equilibrium and none if there are other stable equilibria in the system is clearly contradicted by the maps of Fig. 3.

The complexity of the bifurcation structure evident in Fig. 3b is compounded by the emergence of new types of bifurcation as the cross-infection coefficients β_{12} and β_{21} (i.e., S_{01} and S_{02}) are increased (Greenman and Hudson, 1997b). For simplicity we will suppose that these coefficients are sufficiently low in value that the structure of Fig. 3a is the only new structure to occur within the transcritical framework of Fig. 1c when there is no direct competition.

EXTENDING THE MODEL BY INCLUSION OF DIRECT COMPETITION: BIFURCATION MAP ARRAYS

The bifurcation maps for non-zero values of the direct competition indices v_1 and v_2 can be constructed using the following transformational properties of the linear and hyperbolic transcritical curves. If v_1 is increased from zero up to the “critical” (weak–strong boundary) value of 1 then the transcritical curves move in the following way:

- (i) the vertical asymptote of the hyperbola moves to the vertical axis;
- (ii) the horizontal asymptote moves to the line $R_{02} = 1$;
- (iii) the horizontal L_2 line (if it is active) also moves to the line $R_{02} = 1$;
- (iv) the vertical L_1 line (if it is active) stays fixed; and
- (v) the hyperbola moves towards its asymptotes, collapsing onto them when $v_1 = 1$.

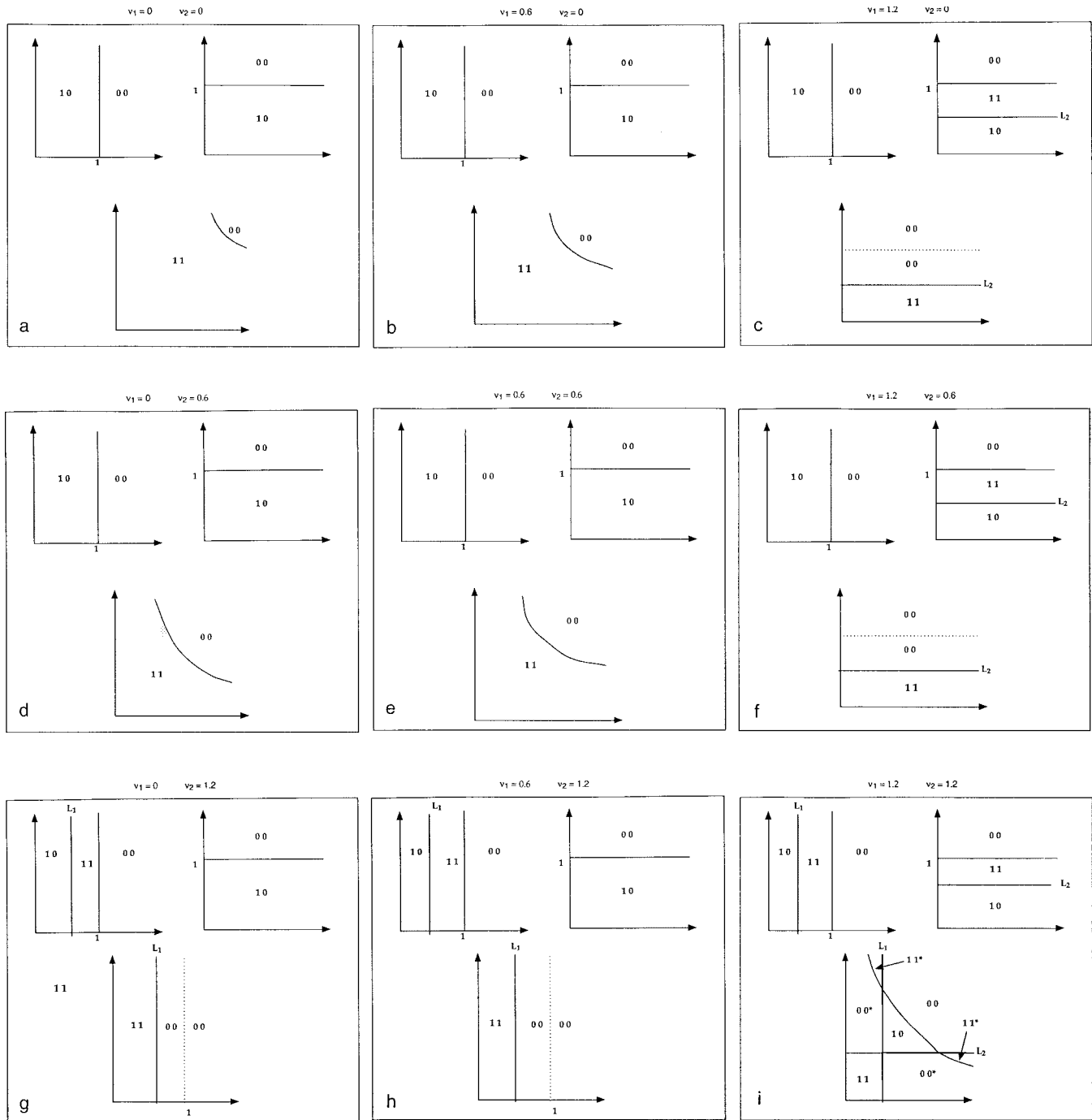


FIG. 4. An array of bifurcation maps for the infected equilibria generated by increasing the dimensionless competition indices v_1 and v_2 from zero. Reading across, v_1 takes values 0, 0.6, and 1.2 as does index v_2 reading down. In each cell there are three maps: top left for the infected host 1 equilibrium; top right for the infected host 2 equilibrium; and bottom for the infected coexistence equilibrium. Neither L_i line is present initially ($v_1 = v_2 = 0$) nor while both competitive forces remain weak. Lines L_i become active when one or both of the competitive forces is strong. For the significance of the asterisk see the text. The array shows that there is always coexistence in the weak-weak competitive situation but when at least one competitive force is strong host exclusion (with or without infection) or infected coexistence is the dominant mode of behaviour. Coefficient values: $c_{11} = 5.1, c_{12} = 5., c_{21} = 5.6, c_{22} = 5.5, c_{31} = 0.75, c_{32} = 0.76,$ and $s_0 = 0.75$.

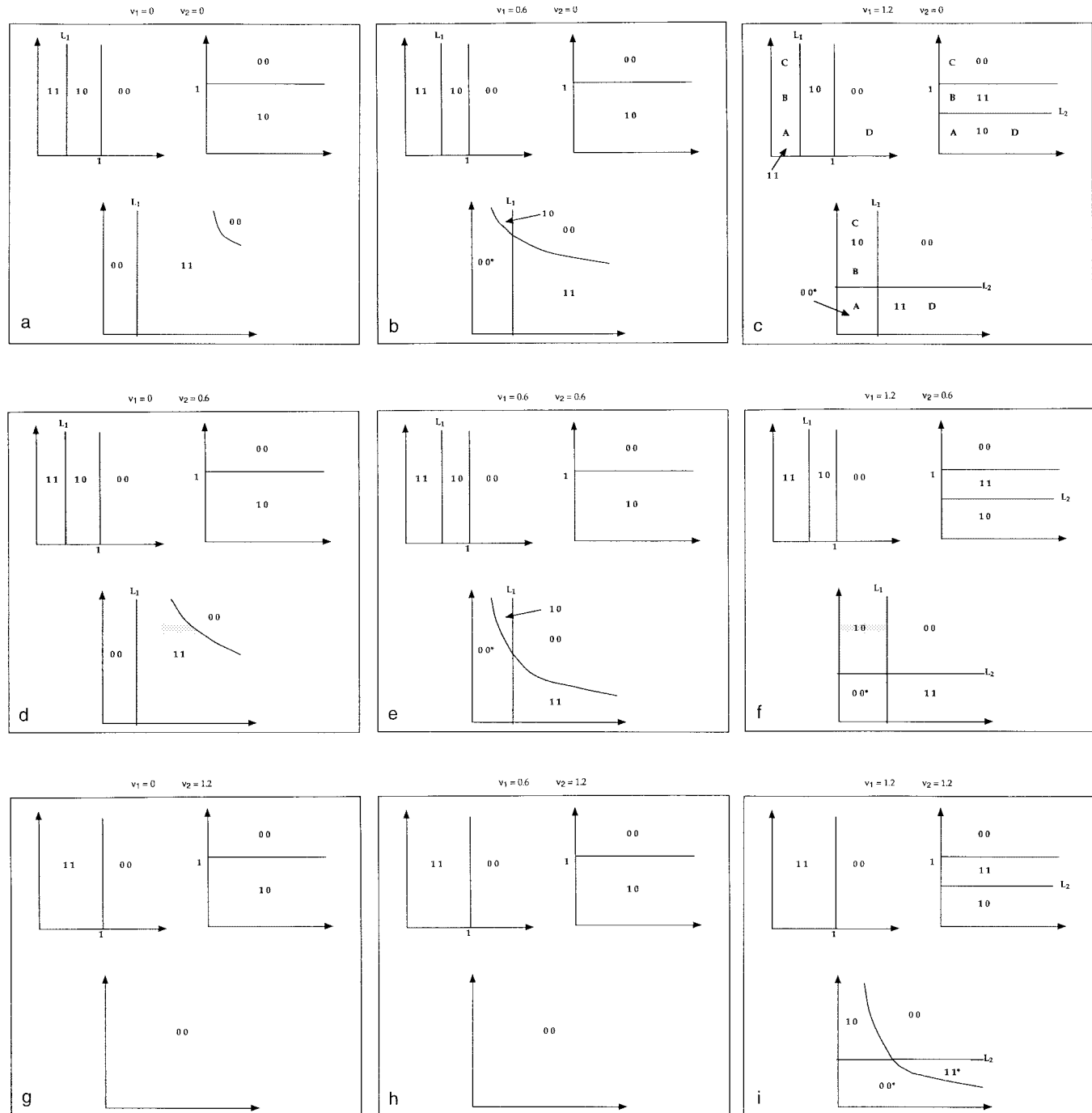


FIG. 5. An array of bifurcation maps when line L_1 is initially active. As v_1 is increased from 0 to 1 (across the array) the vertical asymptote moves to the left to coincide with the vertical axis and the horizontal asymptote to coincide with the line $R_{02}^{-1} = 1$. Line L_1 stays fixed. As v_2 is increased from 0 to 1 (down the array) both L_1 and the vertical asymptote move to coincide with line $R_{01}^{-1} = 1$ while the horizontal asymptote moves to the horizontal axis. In both transitions the hyperbola collapses onto its asymptotes. Note in particular that increasing the competitive force on the host excluded in (a) (i.e., host 2) leads eventually to exclusion (of host 2) in all circumstances (g). Also, increasing the force on the host persisting in (a) (i.e., host 1) leads to a range of possible modes of behaviour (c) discussed in detail in the final section of the main text. Further, comparison of (e) and (i) shows a structural “duality” between strong and weak cases (with respect to transcritical bifurcations). Changing from weak to strong, host $1 \leftrightarrow$ host 2, stable \leftrightarrow unstable takes us from (e) to (i). Coefficient values: $c_{11} = 1.5$, $c_{12} = 2.1$, $c_{21} = 2.0$, $c_{22} = 2.6$, $c_{31} = 0.75$, $c_{32} = 0.76$, and $s_0 = 0.75$.

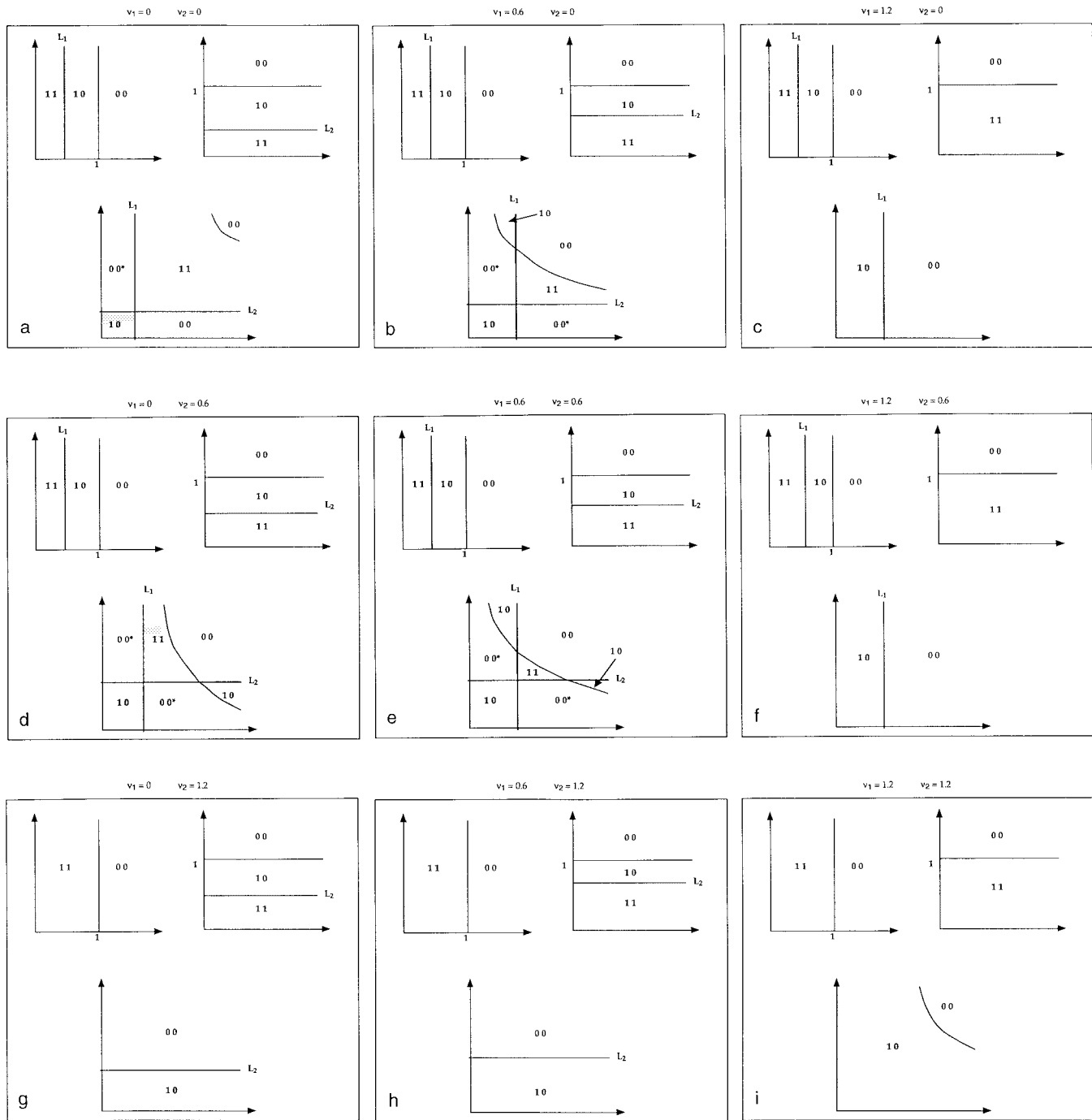
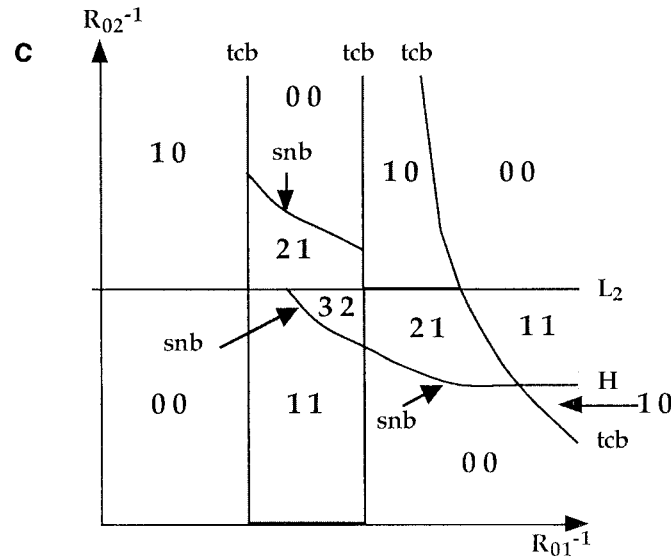
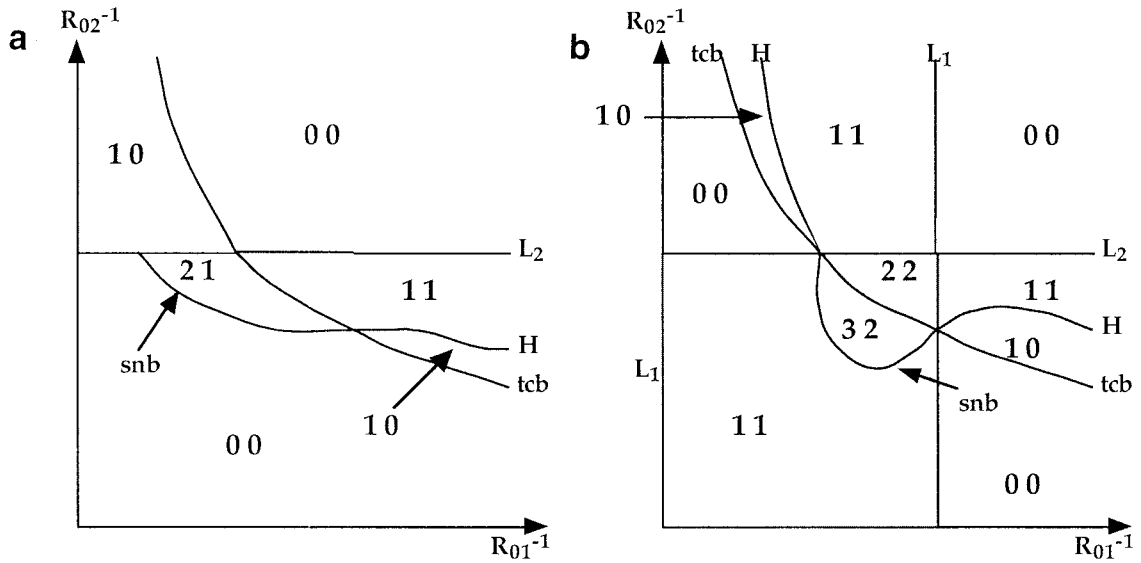


FIG. 6. The array of bifurcation maps when both L_i lines are initially active. Note in particular that, when at least one competitive force is strong, stable coexistence is not possible. This contrasts with the weak-weak situation where infected coexistence is possible within a highly fragmented relevance region. Also, compare (i) with Fig. 4e and (e) with Fig. 4i. Coefficient values: $c_{11} = 1.8$, $c_{12} = 2.1$, $c_{21} = 2.3$, $c_{22} = 2.6$, $c_{31} = 0.8$, $c_{32} = 1.5$, and $s_0 = 0.75$.

Transcritical, Saddle Node and Hopf Bifurcations for the Infected Coexistence Equilibrium



H = Hopf bifurcation snb = saddle node bifurcation
tcb = transcritical bifurcation

FIG. 7. Detail on the infected coexistence bifurcation maps shown in Figs. 4, 5, and 6: (a) The relevance region in Fig. 5i showing the Hopf bifurcation. (b) The strong-strong regime for Fig. 4 when $c_{31} = c_{32} = 0.2$. In this case the hyperbola is lowered sufficiently to intersect the stable relevance region adjacent to the origin. (c) The effect of parallel L_1 lines dissecting the relevance region for the infected coexistence equilibrium. Coefficient values: $c_{11} = 2.05$, $c_{12} = 6.50$, $c_{21} = 6.5$, $c_{22} = 10.95$, $c_{31} = 0.2$, $c_{32} = 0.2$, $s_0 = 0.75$, $v_1 = 1.25$, and $v_2 = 1.25$.

If v_2 rather than v_1 is increased then a similar set of rules holds with “horizontal” replaced by “vertical” and conversely. These rules follow from:

(a) the properties of the L_i lines as functions of v_j ($j \neq i$), established in the Appendix (we are ignoring for the moment the possibility, discussed in the Appendix, of there being multiple parallel L_i lines); and

(b) the form of the equation for the stability boundary of the uninfected coexistence equilibrium when v_1 and v_2 are not both zero,

$$(R_{01}^{-1} - \xi_1)(R_{02}^{-1} - \xi_2) = \xi_1 \xi_2 (\beta_{12} \beta_{21}) / (\beta_{11} \beta_{22})$$

with $\xi_i = (1 - v_i) / (1 - v_1 v_2)$. This is again a hyperbola and clearly reduces to $(3 =)$ when $v_1, v_2 = 0$.

Similar rules can be derived for the strong-weak ($v_i > 1, v_j < 1; j \neq i$) and strong-strong ($v_1, v_2 > 1$) regimes (see the Appendix). In the strong-weak case the rules are simplified by the hyperbola not being active.

With these sets of rules, arrays of bifurcation maps have been constructed in Figs. 4, 5, and 6, describing the change in the map structure as the indices v_i are increased. Each cell in an array is defined by the choice of indices v_1 and v_2 and contains the separate maps for the three infected equilibria. Increasing v_1 (v_2) corresponds to moving horizontally (vertically) through the array. The top left cell in the array corresponds to no direct competition ($v_1 = v_2 = 0$) and the bottom right cell, to strong-strong competition ($v_1, v_2 > 1$). The top left 2×2 inner array of cells corresponds to the weak-weak competitive regime with $0 \leq v_1, v_2 < 1$, and the third column of cells to cases where the competitive force on host 1 is strong ($v_1 > 1$), and the third row to cases where $v_2 > 1$. The three arrays in Figs. 4, 5, and 6 are distinguished by whether the S_{0i} indices are greater or less than 1 in value and hence how many L_i lines are active under the weak-weak regime. In Fig. 4 neither line is active and hence host exclusion is not possible; in Fig. 5 line L_1 is active and hence host 2 can be excluded; in Fig. 6 each host can be excluded.

Adding Saddle-Node and Hopf Bifurcation Structure

For clarity in these maps, we have left out areas where there are multiple infected coexistence equilibria. They occur at the intersection of pairs of transcritical curves. This includes the intersection of an L_i line with the hyperbola as well as L_i lines with each other. These areas expand and merge, with increase in S_{0i} . Also not shown for clarity are curves generated by Hopf bifurcations. In such a bifurcation the real parts of a pair of complex

eigenvalues of the system Jacobian, evaluated at the equilibrium in question, change sign. As a result, the equilibrium becomes unstable if it was previously stable. Hopf bifurcations have to occur for the strong-strong maps of Figs. 4 and 5, otherwise there would be incompatibility with stability switching. To elaborate on this point, if the infected coexistence equilibrium were stable in an area adjacent to the hyperbolic boundary of its relevance region (e.g., Fig. 5i) then in exiting through the uninfected coexistence gate it would transfer that stability to that equilibrium but, as previously stated, the uninfected coexistence equilibrium is never stable in the strong-strong regime. This dilemma is resolved by the existence of a rim of instability adjacent to the hyperbola in the otherwise stable parts of the relevance region of the infected coexistence equilibrium (Fig. 7a). This rim of instability does not remain narrow if the v_i indices are further increased. The area of instability progressively spreads across the previously stable area. The regions of the bifurcation maps where saddle-node or Hopf bifurcations take place are indicated by an asterisk in Figs. 4, 5, and 6.

Hopf bifurcations are of major biological significance, modelling natural systems that exhibit internally driven sustained oscillations. As the Hopf threshold is crossed, previously convergent oscillations become divergent, tending typically to a limit cycle. This form of instability is particularly evident in systems where infection has a major impact on fecundity (Dobson and Hudson, 1992; Hochberg and Holt, 1990).

Hopf and saddle-node bifurcations describe two mechanisms by which the number of relevant stable equilibria in the system can be reduced. They differ in that at a Hopf bifurcation the system is oscillatory (due to dominant imaginary eigenvalues) while at the saddle-node bifurcation the behaviour cannot be oscillatory because the dominant eigenvalue is zero. In this latter case, instability is brought about by the speed of monotonic convergence to equilibrium tending to zero.

DISCUSSION: INTERPRETATION OF THE BIFURCATION MAP ARRAYS

The arrays presented in Figs. 4, 5, and 6 provide a concise catalogue of the possible dynamical modes of the system and the conditions under which they occur. To interpret these arrays we look separately at the situations where host exclusion and coexistence take place. For clarity of exposition we will employ the term “competition,” used without qualification, to refer to direct competition between hosts.

Host Exclusion

These arrays illustrate the fact (see the Appendix) that the stability region of the infected host i equilibrium (i.e., the region of host exclusion with $S_{0i} > 1$) does not contract with increase in either of the competition indices (v_1, v_2) and, in fact, necessarily expands if the competition on the other host increases (e.g., Figs. 5b and 5e, $v_2 \rightarrow 1$). There can, therefore, be host exclusion when previously there was host invasion when the two forces of competition, cross infection (S_{0i}) and direct competition ($v_j; j \neq i$), work together to bring this about.

If there is no host exclusion when competition is weak (e.g., for $S_{02} < 1$ in Figs. 4 and 5) then there can be exclusion when competition is strong, but this will occur with inversion (e.g., Figs. 4c and 5c); i.e., there is exclusion for values of R_{0i} less than rather than greater than a critical value (i.e., above rather than below the L_i line). This inversion is related by stability switching to the fact that the uninfected single-host equilibrium is stable below the infection threshold $R_{0i} < 1$ by competitive exclusion. So, with sufficiently strong competition there can be host exclusion with infection, below the “exclusion” threshold, i.e., for $S_{0i} < 1$.

To illustrate the use of these arrays to determine the characteristics of particular systems, consider the model defined by point A in Fig. 5c. When alone each host exists in a stable infected state. With only competition present, host 1 is excluded; with both infection and competition present, host 2 is excluded. This reversal is similar to the experimental findings on flour beetles made by Park (1948). A better fit is perhaps provided by point C (Fig. 5c) where host 2 is not infected when host 1 is absent. In this case the system possesses a pair of stable states with either host 1 infected (and host 2 excluded) or host 2 uninfected (and host 1 excluded). The state with host 2 excluded is therefore not the only stable “solution.” Which state is chosen depends on the initial conditions. Finally, we note that at point B in Fig. 5c the choice is between two stable infected single-host equilibria when both infection and competition are present.

Exclusion inversion is also a key component of the duality relationship evident in the stability structure of the infected single-host equilibria. This duality is realised by switching between (i) strong and weak exclusion ($(S_{0i} < 1) \leftrightarrow (S_{0i} > 1); i = 1, 2$), (ii) strong and weak competition ($(v_i > 1) \leftrightarrow (v_i < 1); i = 1, 2$), and (iii) stability and instability (Figs. 4, 5, and 6). For example, if these switches are made then Fig. 4i becomes Fig. 6e and Fig. 5e becomes Fig. 5i. Because the infected coexistence relevance region is constructed in part from

the single-host bifurcation structures this duality is also reflected in the infected coexistence bifurcation maps.

Coexistence

In the case of weak–weak competition the dominant effect evident in the arrays of Figs. 4, 5, and 6 is the expansion of the stability region for the uninfected coexistence equilibrium with an increase in the strength of competition. Because of this expansion it is possible for the uninfected coexistence stability region to overlap not only the regions of relevance for the infected single-host equilibria but also their regions of stability. In the latter case it is possible for the system to possess both a stable uninfected coexistence equilibrium and a stable infected single-host equilibrium (Figs. 5 and 6; b and e), a fact noted also by Bowers and Turner (1997). If

$$1 > v_1 v_2 > p > 0, \quad \text{where} \quad p = (\beta_{12}\beta_{21})/(\beta_{11}\beta_{22}), \quad (4)$$

then the uninfected coexistence stability region overlaps the region where both infected single-host equilibria are relevant but not stable. As a result (i) it is possible for the uninfected coexistence equilibrium to be stable when neither host can resist pathogen or host invasion (Figs. 4e and 5e) and (ii) the uninfected coexistence equilibrium is always stable when both hosts can resist pathogen invasion. It should be noted that condition (4) cannot hold in the weak–weak competition regime when both hosts are above the exclusion threshold (i.e., $S_{0i} > 1$, Fig. 6) since then $p > 1$, nor in the no-competition case.

In the regime where there is strong–strong competition ($v_i > 1, i = 1, 2$) the uninfected coexistence equilibrium is relevant but unstable while the infected coexistence equilibrium is either unstable when relevant (Fig. 6) or fragmented into stable and unstable regions (Figs. 4i and 5i). If p (in (4)) has a sufficiently low value it is possible for the hyperbola to intersect the stable region containing the origin (Fig. 7b) and the infected coexistence equilibrium is then always stable when relevant, except for the Hopf rims. When infection transmission is not too strong (i.e., at least one S_{0i} less than 1) infection acts as the glue to establish stable coexistence but the fragmentation shows that this cannot always be achieved.

In the weak–strong competition regime ($v_i > 1, v_j < 1 (j \neq i)$) the uninfected coexistence equilibrium is not relevant but the infected coexistence equilibrium can be not only relevant but also stable (Figs. 4 and 5). One implication of this is the possibility of infection allowing the invasion of a host previously competitively excluded. Consider the point D in Fig. 5c. When both hosts are

alone they each support the pathogen; in the absence of infection host 1 is excluded; with both infection and competition present the hosts coexist with the infection. This might be what is happening in the invasion of the European mussel, *Mytilus galloprovincialis*, discussed in the Introduction (Calvo-Ugarteburu and McQuaid, 1997) although the evidence remains circumstantial.

One interesting property of the competition-extended S-I model is, as we have noted, the possibility of pairs of stable equilibria, involving both coexistence and single-host equilibria and both infected and uninfected equilibria, occurring even when only transcritical bifurcations are considered. If saddle-node and Hopf bifurcation structure is added then the possible combinations of stable equilibria increase with (i) multiple stable infected coexistence equilibria, (ii) stable infected single-host and coexistence equilibria, and (iii) no stable equilibria at all (Greenman and Hudson, 1997b).

To add further complexity, it is shown in the Appendix how multiple L_i lines can be generated in certain bounded regions of parameter space. This leads to high fragmentation of the infected coexistence relevance region and the creation of a large number of bifurcation curve intersections. A typical outcome is shown in Fig. 7c, generated by a mix of transcritical, saddle-node, and Hopf bifurcations with a triplet of infected coexistence equilibria occurring in one of the relevance subregions. It is also possible, in a restricted part of parameter space with weak competitive forces operating ($S_{0i} < 1$, $v_j < 1$; $j \neq i$), to generate a pair of parallel L_i lines and thereby create a region of stability in an otherwise unstable region for the infected host i equilibrium. This provides a second example where host exclusion is possible below the exclusion threshold $S_{0i} = 1$.

It should also be borne in mind that the arrays of Figs. 5 and 6 have been constructed from the maps that have the simplest structure when direct competition is absent. More complicated maps, involving a richer bifurcation structure (Greenman and Hudson, 1997b), could have been chosen for the base maps of Figs. 5a and 6a and this extra complexity would have cascaded through the arrays.

The analysis has been restricted to the microparasite S-I model and its extensions. We are also examining the effect of the interplay of competitive forces in macroparasite models (Dobson and Hudson, 1992), using the methods described in this paper. It is only the situation of Fig. 5 with one L_i line active that is possible in this macroparasite case. We are also looking at single-host multi-parasite systems where the map structures appear to be more complex but the bifurcation methods we have been using are sufficiently flexible to handle the new structures.

APPENDIX

Stability (with Respect to the Other Host) for the Infected Single-Host Equilibria

At the infected host 1 equilibrium the dimensionless state variable $h_1 = H_1/K_1$ satisfies the quadratic equation

$$R_{01}^{-1} = (h_1/c_{11})(h_1 + c_{11} - 1) = F(h_1) \quad (0 \leq h_1 \leq 1) \quad (\text{A1})$$

and $y_1 = (\beta_{11}/d_1) Y_1$ is given, in terms of h_1 , by

$$y_1 = h_1(1 - h_1)/(c_{11}R_{01}^{-1}) = h_1R_{01} - 1. \quad (\text{A2})$$

The condition for stability against invasion by host 2 has the form

$$c_{31}y_1(c_{12} + v_2h_1 - 1) > (1 - v_2h_1). \quad (\text{A3})$$

(Coefficients c_{1i} and c_{3i} are defined in Table I.) (For derivation see Bowers and Turner, 1997.) Eliminating R_{01} and y_1 between (A1), (A2), and (A3), we obtain the inequality

$$Q(h_1, v_2) > 0, \quad (\text{A4})$$

where Q is the quadratic function

$$\begin{aligned} Q(h_1, v_2) = & h_1^2 v_2 (1 - c_{31}) + h_1 (c_{31} (v_2 - (c_{12} - 1)) \\ & - (1 - v_2 (c_{11} - 1))) \\ & + c_{31} (c_{12} - 1) - (c_{11} - 1). \end{aligned} \quad (\text{A5})$$

To determine for what range of R_{01}^{-1} there is host exclusion with infection we first note the following facts: (i) (A1) gives a 1-1 mapping from h_1 to R_{01}^{-1} in the relevance region $0 \leq h_1 \leq 1$ and (ii) at the endpoints $h_1 = 0, 1$ function Q takes the values

$$Q(0, v_2) = (c_{11} - 1)(S_{01} - 1)$$

$$\text{and } Q(1, v_2) = c_{11}(v_2 - 1).$$

If these end values have opposite sign there is one and only one solution to Eq. (A4) with equality. We conclude that when $S_{01} > 1$, $v_2 < 1$ there is exclusion in the interval

$$R_{01}^{-1} < R_{01}^{*-1} < 1,$$

$$\text{where } R_{01}^{*-1} = F(q_1), \quad Q(q_1, v_2) = 0$$

and when $S_{01} < 1$, $v_2 > 1$ there is exclusion in the interval $R_{01}^{*-1} < R_{01}^{-1} < 1$; i.e., there is exclusion inversion. (Note that the equation for the L_1 line is $R_{01} = R_{01}^*$.) If the end values of Q are of the same sign then it is possible for there to be no solution to (A4) with equality or two solutions. In the former case when $S_{01} < 1$, $v_2 < 1$ there can be no host exclusion and when $S_{01} > 1$, $v_2 > 1$ there is always exclusion above the threshold $R_{01} > 1$. When there are two solutions and when $S_{01} < 1$, $v_2 < 1$ there can be exclusion for the interval $0 < q_1 < h_1 < q_2 < 1$, where $Q(q_i, v_2) = 0$. For this to happen it must be that

$$1 > S_{01} > \max(1, c_{11}/c_{12}) * (c_{12} - 1)/(c_{11} - 1)$$

and v_2 cannot be too small, since, when $v_2 = 0$, Q is linear in h_1 . When there are two solutions and $S_{01} > 1$, $v_2 > 1$, then there can be an interval excised from the host exclusion interval; i.e., there is exclusion when either $0 < h_1 < q_1$ or $q_2 < h_1 < 1$ with $q_1 < q_2$ and $Q(q_i, v_2) = 0$. For this to happen it must be that

$$1 < S_{01} < \min(1, c_{11}/c_{12}) * (c_{12} - 1)/(c_{11} - 1)$$

and v_2 cannot be too large.

From this analysis two results are particularly useful:

(a) The region of stability (i.e., the interval for which $Q > 0$) expands with increase in v_2 since Q is linear in v_2 with positive coefficient (see (A5)).

(b) The condition $S_{01} < 1$ preventing host exclusion can fail when there are two solutions to $Q = 0$ in the interval $0 \leq h_1 \leq 1$ and does fail when competition is strong ($v_2 > 1$).

ACKNOWLEDGMENTS

We gratefully acknowledge useful discussions with Roger Bowers, Andy Dobson, Bryan Grenfell, and others. We also acknowledge the use of the computer program "Mathematica" in carrying out the numerical and algebraic calculations.

REFERENCES

Allison, A. C. 1982. Coevolution between hosts and infectious disease agents, and its effects on virulence, in "Population Biology of Infectious Diseases" (R. M. Anderson and R. M. May, Eds.), pp. 245–267, Springer-Verlag, Berlin/New York.

Anderson, R. M., and May, R. M. 1986. The invasion, persistence and spread of infectious diseases within animal and plant communities, *Philos. Trans. R. Soc. London B* **314**, 533–570.

Anderson, R. M., and May, R. M. 1991. "Infectious Diseases of Humans: Dynamics and Control," Oxford Univ. Press, Oxford.

Begon, M., and Bowers, R. G. 1992. Disease and community structure: The importance of host self-regulation in a host–pathogen model, *Am. Nat.* **139**, 1131–1150.

Begon, M., and Bowers, R. G. 1994. Host–host–pathogen models and microbial pest control: The effect of host self-regulation, *J. Theor. Biol.* **169**, 275–287.

Begon, M., and Bowers, R. G. 1995. Beyond host–pathogen dynamics, in "Ecology of Infectious Diseases in Natural Populations" (B. T. Grenfell and A. P. Dobson, Eds.), pp. 478–509, Cambridge Univ. Press, Cambridge, UK.

Bonsall, M. B., and Hassell, M. P. 1997. Apparent competition structures of ecological assemblages, *Nature* **388**, 371–373.

Bowers, R. G., and Turner, J. 1997. Community structure and the interplay between interspecific infection and competition, *J. Theor. Biol.* **187**, 95–109.

Broekhuizen, S., and Kememrs, R. 1976. The stomach worm, *Graphidium strigousum* (Dujardin), in the European hare, *Lepus europaeus*, Pallas, in "Ecology and Management of European Hare Populations" (Z. Pielowski and Z. Pucek, Eds.), Polish Hunt Soc., Warsaw.

Calvo-Ugarteburu, G., and McQuaid, C. D. 1997. Parasitism and introduced species: Epidemiology of trematodes in the intertidal mussels *Perna perna* and *Mytilus galloprovincialis*, *J. Exp. Mar. Biol. Ecol.* **120**, 47–65.

Dobson, A. P., and Hudson, P. J. 1992. Regulation and stability of a free-living host–parasite system: *Trichostrongylus tenuis* in red grouse. II. Population models, *J. Anim. Ecol.* **61**, 487–498.

Greenman, J. V., and Hudson, P. J. 1997a. Infected coexistence instability with and without density-dependent regulation, *J. Theor. Biol.* **185**, 345–356.

Greenman, J. V., and Hudson, P. J. 1997b. "Exploring the Complexity of Parasite-Mediated Competition Using Gateway Analysis," Stirling Mathematical Ecology Group Working Paper No. 10.

Greenman, J. V., and Hudson, P. J. 1997c. "Competition vs Infection in Macroparasite Multi-host Models," Stirling Mathematical Ecology Group, Working Paper No. 11.

Grenfell, B. T., and Dobson, A. P. (Eds.), 1995. "Ecology of Infectious Diseases in Natural Populations," Cambridge Univ. Press, Cambridge.

Hochberg, M. E., and Holt, R. D. 1990. The coexistence of competing parasites. I. The role of cross-species infection, *Am. Nat.* **136**, 517–541.

Holt, R. D., and Lawton, J. H. 1994. The ecological consequences of shared natural enemies, *Annu. Rev. Ecol. Syst.* **25**, 495–520.

Holt, R. D., and Pickering, J. 1985. Infectious diseases and species coexistence: A model of Lotka–Volterra form, *Am. Nat.* **126**, 196–211.

Hudson, P. J., and Greenman, J. V. 1998. Competition mediated by parasites: Biological and theoretical progress, *TREE* **13**, 387–390.

MacDonald, D. W. 1993. Rabies and wildlife: A conservation problem? *Onderstepoort J. Vet. Res.* **60**, 351–355.

Murray, J. D. 1993. "Mathematical Biology," Springer-Verlag, Berlin/New York.

Park, T. 1948. Experimental studies of interspecific competition. I. Competition between populations of the flour beetles, *Tribolium confusum* and *Tribolium castaneum*, *Ecol. Monogr.* **18**, 267–307.

Scott, M. E., and Smith, G. 1994. "Parasitic and Infectious Disease," Academic Press, New York.

Wiggins, S. 1990. "Introduction to Applied Nonlinear Dynamical Systems and Chaos," Springer-Verlag, Berlin/New York.

Yan, G. 1996. Parasite-mediated competition: A model of directly transmitted macroparasites, *Am. Nat.* **148**, 1089–1112.